Research Article

Approximate solution for a system of fractional integro-differential equations by Müntz Legendre wavelets

Y. Barazandeh

Abstract

We use the Müntz Legendre wavelets and operational matrix to solve a system of fractional integro-differential equations. In this method, the system of integro-differential equations shifts into the systems of the algebraic equation, which can be solved easily. Finally, some examples confirming the applicability, accuracy, and efficiency of the proposed method are given.

1 Introduction

The theory of fractional calculus and especially fractional differential equations has recently become a popular topic, and many natural phenomena are modeled by it in [26, 21, 28, 11, 17, 2, 3]. The fractional integro-differential equations (FIDEs) are generalized integro-differential equations. In general, it is very difficult to obtain an exact solution for most FIDEs, so the use of approximate methods seems necessary. Many studies have used approximate methods to solve FIDE problems, such as Adomian decomposition method [9, 18], variational iteration method [10, 29, 22], the generalized differential transform method [1, 23], the homotopy perturbation method [36, 27], the collocation method [12, 19, 14, 34, 16], and block-pulse functions (BPFs) method [4, 7, 32, 33].

One type of the numerical methods that has been used effectively for solving FIDEs is wavelets methods, which can be referred to in as Legendre

Yousef Barazandeh
Department of Mathematics, Lorestan University, Khorramabad, Iran.
e-mail: barazandeh.yu@fs.lu.ac.ir

wavelets [35], Chebyshev wavelets [37], Haar wavelets [31], Bernoulli wavelet [13, 30], and Müntz Legendre wavelets [5]. Consider the following nonlinear system of FIDEs, where $s, t \in [0,1], 0 < p, q \leq 1$, and D^p and D^q represent Caputo derivative:

$$\begin{cases} D^p y_1(t) = f_{11}(t, y_1(t), y_2(t)) + \int_0^t f_{12}(s, y_1(s), y_2(s))ds, \\ D^q y_2(t) = f_{21}(t, y_1(t), y_2(t)) + \int_0^t f_{22}(s, y_1(s), y_2(s))ds. \end{cases} \quad (1)$$

In this article, Müntz Legendre wavelets and operational matrix have been used to obtain a numerical solution for relation (1).

The organization of the paper is as follows: In Section 2, some basic results from the fractional calculus and the definition of Müntz Legendre wavelets are given. In Section 3, a numerical method based on Müntz Legendre wavelets for an approximation system of FIDEs and its convergence analysis is presented. In Section 4, the mentioned method has been examined by some examples. Finally, the conclusion is given in Section 5.

2 Preliminaries

In this section, some basic results from the fractional calculus and Müntz polynomial are given.

2.1 Caputo derivative and Riemann–Liouville integral

Definition 1 (see [25])**.** The fractional derivative of $f(t)$ in Caputo sense for $p, t \in [0,1]$ is defined as

$$D^p f(t) = \frac{1}{\Gamma(1-p)} \int_0^t (t-\tau)^{-p} f'(\tau)d\tau,$$

where $f(t)$ is an unknown function in an appropriate functional space and Γ is the gamma function.

Definition 2 (see [25])**.** The Riemann–Liouville fractional integral of order p can be defined as follows:

$$I^p f(t) = \frac{1}{\Gamma(p)} \int_0^t (t-s)^{p-1} f(s)ds.$$

Remark 1 (see [25])**.** The following relationships exist between Caputo derivative and Riemann–Liouville integral:

$$D^p I^p f(t) = f(t),$$

$$I^p D^p f(t) = f(t) - \sum_{m=0}^{n-1} \frac{f^{(m)}(0^+)}{m!} t^m, \qquad t \geq 0, \quad n-1 < p < n. \qquad (2)$$

2.2 Müntz polynomial and Müntz Legendre wavelets

Theorem 1 (see [24]). The sequence $\{t^{\lambda_i}\}_{i=0}^{\infty}$, with $0 \leq \lambda_0 < \lambda_1 < \cdots \to \infty$ is fundamental in $L_2[0,1]$ if and only if

$$\sum_{k=1}^{\infty} \lambda_k^{-1} = \infty.$$

The classical Müntz polynomial is represented as

$$\sum_{k=0}^{N} a_k t^{\lambda_k},$$

where $a_k \in \mathbb{R}$.
The Müntz Legendre polynomial is an orthogonalized Müntz polynomial respect to the Lebesgue measure in $[0,1]$. Assume that $\Lambda_n = \{\lambda_0, \lambda_1, \lambda_2, \ldots, \lambda_n\}$ and that

$$Re(\lambda_k) > -\frac{1}{2} \quad (k \in \mathbb{N}_0), \quad \lambda_k \neq \lambda_j \; (k \neq j).$$

Then we can represent Müntz Legendre polynomial as follows (see [8, 20]):

$$\mathcal{L}_n(t) = \sum_{k=0}^{n} c_{k,n} t^{\lambda_k}, \qquad c_{k,n} = \frac{\prod\limits_{j=0}^{n-1}(\lambda_k + \lambda_j + 1)}{\prod\limits_{j=0,j\neq k}^{n}(\lambda_k - \lambda_j)} \qquad (n \in \mathbb{N}_0).$$

In this paper, we set $\lambda_k = k\gamma$ and $\gamma = 1$.

Müntz Legendre wavelets are defined on $[0,1]$ as (see [5]):

$$\varphi_{nm}(t) = \begin{cases} \sqrt{2^{k-1}(1+2m\gamma)} + \mathcal{L}_m(2^{k-1}t - n - 1, \gamma), & \dfrac{n-1}{2^{k-1}} \leq t < \dfrac{n}{2^{k-1}}, \\ 0 & \text{otherwise,} \end{cases}$$

where $n = 1, 2, \ldots, 2^{k-1}$, $m = 0, 1, 2, \ldots, M-1 (k, M \in \mathbb{N})$, and $\mathcal{L}_m(t, \gamma)$ is the well-known Müntz Legendre of order m, that in which $\lambda_k = k\gamma$.

3 Approximation of function by using Müntz Legendre wavelets

Any function y belonging to $L_2[0,1]$ can be expanded by Müntz Legendre wavelets as follows (see [5]):

$$y(t) \simeq \sum_{n=1}^{\infty} \sum_{m=0}^{\infty} a_{nm} \varphi_{nm}(t). \tag{3}$$

Assume that

$$\{\varphi_{1,0}(t), \ldots, \varphi_{1,M-1}(t), \varphi_{2,0}(t), \ldots, \varphi_{2,M-1}(t), \ldots,$$
$$\varphi_{2^{k-1},0}(t), \ldots, \varphi_{2^{k-1},M-1}(t)\}$$

is a set of Müntz Legendre wavelets and that

$$\mathrm{X} = \mathrm{span}\{\varphi_{1,0}(\mathrm{t}), \ldots, \varphi_{1,M-1}(\mathrm{t}), \varphi_{2,0}(\mathrm{t}), \ldots, \varphi_{2,M-1}(\mathrm{t}), \ldots,$$
$$\varphi_{2^{k-1},0}(t), \ldots, \varphi_{2^{k-1},M-1}(t)\}.$$

Since X is a finite-dimensional function space of $L_2[0,1]$, so y has the best unique approximation $y_{m'} \in \mathrm{X}$ such that $||y - y_{m'}|| \leq ||y - x||$ for all $x \in \mathrm{X}$. Moreover, there are unique coefficients a_{nm} such that

$$y(t) \simeq y_{m'} = \sum_{n=1}^{2^{k-1}} \sum_{m=0}^{M-1} a_{nm} \varphi_{nm}(t) = A_{nm}^{T} \Phi_{nm}(t), \tag{4}$$

where

$$A_{nm} = \left[a_{1,0}, \ldots, a_{1,M-1}, a_{2,0}, \ldots, a_{2,M-1}, \ldots, a_{2^{k-1},0}, \ldots, a_{2^{k-1},M-1} \right]^{T},$$

$$\Phi_{nm}(t) = \left[\varphi_{1,0}(t), \ldots, \varphi_{1,M-1}(t), \varphi_{2,0}(t), \ldots, \varphi_{2,M-1}(t), \ldots \right.$$
$$\left. \varphi_{2^{k-1},0}(t), \ldots, \varphi_{2^{k-1},M-1}(t) \right]^{T}.$$

Equation (4) can be rewritten as

$$y(t) \simeq y_{m'}(t) = \sum_{i=1}^{m'} a_i \varphi_i(t) = A_{m'}^{T} \Phi_{m'}(\mathrm{t}), \tag{5}$$

where

$$A_{m'} = \left[a_1, \ldots, a_M, a_{M+1}, \ldots, a_{2M}, \ldots a_{2^{k-1}(M+1)}, \ldots, a_{m'} \right]^{T},$$

$$\Phi_{m'} = \left[\varphi_1(t), \ldots, \varphi_M(t), \varphi_{M+1}(t), \ldots, \varphi_{2M}(t), \ldots \varphi_{2^{k-1}(M+1)}(t), \ldots, \varphi_{m'}(t) \right]^T,$$

$$a_i = a_{nm}, \quad \varphi_i = \varphi_{nm}, \quad i = (n-1)M + m + 1, \quad m' = 2^{k-1}M.$$

Suppose that $t_i = \frac{2i-1}{2m'}$, $i = 1, 2, 3, \ldots, m'$ are collocation points. We define the Müntz Legendre wavelets Ψ as follows:

$$\Psi_{m' \times m'} = \left[\Phi(\frac{1}{2m'}) \ \ \Phi(\frac{3}{2m'}) \ \ \Phi(\frac{5}{2m'}) \ \ \cdots \ \ \Phi(\frac{2m'-1}{2m'}) \right].$$

Theorem 2 (see [6]). Suppose that $y(t) \in \mathbb{C}^M[0,1]$. that $y_{m'}(t) \in \mathrm{X}$ is the approximation of $y(t)$ via wavelet, and that there exists $D \in \mathbb{N}$ such that $|y^{(M)}(t)| < D$ for all $t \in [0,1]$. Then

$$\|e_y\| = \|y(t) - y_{m'}(t)\| \leq \frac{D}{M! 2^{M(k-1)}}.$$

Theorem 3. Suppose that in (1), f_{ij} $(i, j = 1, 2)$ satisfies the Lipschitz condition and $y_{i_{m'}}$ is an approximate solution of $y_i(t)$ by the Müntz Legendre wavelets method. If $k, M \to \infty$, then $\|e_i\| = \|y_i - y_{i_{m'}}\| \to 0$.

Proof. Let $r_i(t)$ $(i = 1, 2)$ be perturbation terms and let $\lceil p_i \rceil = m_i$. we can write $y_{i_{m'}}$ and $y_{i_{m'}} + e_i$ as follows:

$$y_{i_{m'}}(t) = r_i(x) + \sum_{k=1}^{m_i-1} \frac{y_i^{(k)}}{k!} t^k + \frac{1}{\Gamma(p_i)} \int_0^t (t-x)^{p_i-1} f_{i1}(x, y_{1_{m'}}(x), y_{2_{m'}}(x)) dx$$

$$+ \frac{1}{\Gamma(p_i)} \int_0^t \int_0^x (t-x)^{p_i-1} f_{i2}(s, y_{1_{m'}}(s), y_{2_{m'}}(s)) ds dx,$$
$$(6)$$

$$y_{i_{m'}}(t) + e_i(t) = \sum_{k=1}^{m_i-1} \frac{y_i^{(k)}}{k!} t^k$$

$$+ \frac{1}{\Gamma(p_i)} \int_0^t (t-x)^{p_i-1} f_{i1}(x, y_{1_{m'}}(x) + e_1(x), y_{2_{m'}}(x)) + e_2(x) dx$$

$$+ \frac{1}{\Gamma(p_i)} \int_0^t \int_0^x (t-x)^{p_i-1} f_{i2}(s, y_{1_{m'}}(s)$$

$$+ e_1(s), y_{2_{m'}}(s) + e_2(s)) ds dx.$$
$$(7)$$

By subtracting (6) from (7) and employing the Lipschitz condition, we have

$$\|e_i\| \leq \|r_i\| + \frac{1}{\Gamma(p_i)} L_1(\|e_1\| + \|e_2\|) \int_0^t (t-x)^{p_i-1} dx$$

$$+ \frac{1}{\Gamma(p_i)} L_1(\|e_1\| + \|e_2\|) \int_0^t \int_0^x (t-x)^{p_i-1} ds dx.$$
$$(8)$$

By setting $\max\{L_1, L_2\} = L$, $|y_i^{(M)}(t)| < D_i (i = 1, 2)$, $D = \max\{D_1, D_2\}$ and using Theorem 1, we can write

$$
\begin{aligned}
\|e_i\| &\leq \|r_i\| + L(\|e_1\| + \|e_2\|)(\frac{1}{\Gamma(p_i + 1)} + \frac{1}{\Gamma(p_i + 2)}) \\
&\leq \|r_i\| LD \frac{1}{M!2^{M(k-1)}}(\frac{1}{\Gamma(p_i + 1)} + \frac{1}{\Gamma(p_i + 2)}).
\end{aligned}
\tag{9}
$$

Since $k, M \to \infty$, then $\|r_i\| \to 0$. We can conclude that $\|e_i\| \to 0$ ($i = 1, 2$).   □

3.1 Operational matrix of the fractional integration

In this section, we review the fractional-order operational matrix of integration related to the Müntz Legendre wavelets. For this purpose, the required definitions and lemmas are given from [30].

Definition 3. For $m' = 2^{k-1}M$ and $i = 1, 2, \ldots, m'$, the set of BPFs is defined as

$$
\hat{b}_i(t) = \begin{cases} 1, & \frac{(i-1)}{m'} \leq t < \frac{i}{m'}, \\ 0 & \text{otherwise.} \end{cases}
$$

We use the following properties of BPFs:

$$
\hat{b}_i(x)\hat{b}_j(x) = \begin{cases} \hat{b}_i(x), & i = j, \\ 0, & i \neq j, \end{cases}
$$

$$
\int_0^x \hat{b}_i(x)\hat{b}_j(x)dx = \begin{cases} \frac{1}{m'}, & i = j, \\ 0, & i \neq j. \end{cases}
$$

Definition 4. Suppose that $U = [u_1, u_2, \ldots, u_{m'}]^T$ and $V = [v_1, v_2, \ldots, v_{m'}]^T$. We define

$$
U \otimes D = [u_1 v_1, u_2 v_2, \ldots, u_{m'} v_{m'}]^T.
$$

Lemma 1. Let $\hat{B}_{m'} = [\hat{b}_1, \hat{b}_2, \ldots, \hat{b}_{m'}]^T$, and suppose that $f(t), g(t) \in L_2[0, 1]$ can be written as $f(t) = F^T \hat{B}_{m'}(t)$ and $g(t) = G^T \hat{B}_{m'}(t)(F^T = [f_1, f_2, \ldots, f_{m'}], G^T = [g_1, g_2, \ldots, g_{m'}])$. Then

$$
f(x)g(x) \approx F^T \hat{B}_{m'}(t) G^T \hat{B}_{m'}(t) = (F^T \otimes G^T)\hat{B}_{m'}(t),
\tag{10}
$$

$$
f(x)^2 \approx (F^T \hat{B}_{m'}(t))^2 = (F^T)^2 \hat{B}_{m'}(t).
\tag{11}
$$

The Riemann–Liouville fractional integration of order α of BPFs can be presented as (see [15]):

$$I^p \hat{B}_{m'}(t) \approx \mathcal{F}^p \hat{B}_{m'}(t), \tag{12}$$

where $\mathcal{F}^p$ is the BPFs operational matrix with

$$\mathcal{F}^p = \left(\frac{1}{m'}\right)^p \frac{1}{\Gamma(p+2)} \begin{bmatrix} 1 & f_1 & f_2 & \cdots & f_{m'-1} \\ 0 & 1 & f_1 & \cdots & f_{m'-2} \\ 0 & 0 & 1 & \cdots & f_{m'-3} \\ 0 & 0 & 0 & \cdots & f_{m'-4} \\ \vdots & \vdots & \vdots & \ddots & \vdots \\ 0 & 0 & 0 & \cdots & 1 \end{bmatrix},$$

in which $f_k = (k+1)^{p+1} - 2k^{p+1} + (k-1)^{p+1}$, $k = 1, 2, \ldots, m'-1$.

We now derive the operational matrix of fractional integration of Müntz Legendre wavelets. The integration of Müntz Legendre wavelets $\Phi_{m'}(x)$ can be expressed as

$$I\Phi_{m'}(t) = \int_0^t \Phi_{m'}(s)ds \approx \mathcal{P}_{m'}\Phi_{m'}(t), \tag{13}$$

where the m'-square matrix $\mathcal{P}_{m'}$ is called Müntz Legendre wavelets operational matrix. Also

$$I^p\Phi_{m'}(t) \approx \mathcal{P}_{m'}^p \Phi_{m'}(t), \tag{14}$$

where $\mathcal{P}_{m'}^p$ is called Müntz Legendre wavelets fractional integral operational matrix.

The Müntz Legendre wavelets can be expanded into m'-set BPFs as

$$\Phi_{m'}(t) \approx \Psi_{m'} \hat{B}_{m'}(t). \tag{15}$$

Considering (12), we can write (14) and (15) as

$$I^p\Phi_{m'}(t) \approx I^p\Psi_{m'}\hat{B}_{m'}(t) = \Psi_{m'}I^p\hat{B}_{m'}(t) \approx \Psi_{m'}\mathcal{F}^p\hat{B}_{m'}(t),$$

$$\mathcal{P}_{m'}^p\Phi_{m'}(t) \approx I^p\Phi_{m'}(t) \approx \Psi_{m'}\mathcal{F}^p\hat{B}_{m'}(t) \approx \Psi_{m'}\mathcal{F}^p\Psi_{m'}^{-1}\Phi_{m'}(t).$$

Finally, we conclude

$$\mathcal{P}_{m'}^p \approx \Psi_{m'}\mathcal{F}^p\Psi_{m'}^{-1}.$$

4 Examples

In this section, some examples are solved by using the proposed method with different parameters.

Example 1. Consider

$$\begin{cases} D^{\frac{1}{2}}y_1(t) = \Gamma(\frac{3}{2}) + \int_0^t [y_1(s) + y_2(s)]ds, \\ D^{\frac{1}{2}}y_2(t) = y_1(t) + y_2(t) - \Gamma(\frac{3}{2}), \end{cases} \tag{16}$$

where $y_1(0) = 0, y_2(0) = 0$.

Exact solutions for system (16) are $y_1(t) = \sqrt{t}$ and $y_2(t) = -\sqrt{t}$. Indeed

$$D^{\frac{1}{2}}y_1(t) \approx G_{m'}^T \Phi_{m'}(t), \quad D^{\frac{1}{2}}y_2(t) \approx H_{m'}^T \Phi_{m'}(t), \tag{17}$$

where

$$G_{m'}^T = [g_1, g_2, g_3, \ldots, g_{m'}], \quad H_{m'}^T = [h_1, h_2, h_3, \ldots, h_{m'}].$$

By using the initial conditions and (2), (14), (15), and (17), we have

$$\begin{cases} y_1(t) = I^{\frac{1}{2}} D^{\frac{1}{2}} y_1(t) + y_1(0) \approx G_{m'}^T \mathcal{P}_{m'}^{\frac{1}{2}} \Phi_{m'}(t) \approx G_{m'}^T \mathcal{P}_{m'}^{\frac{1}{2}} \Psi_{m'} \hat{B}_{m'}(t), \\ y_2(t) = I^{\frac{1}{2}} D^{\frac{1}{2}} y_2(t) + y_2(0) \approx H_{m'}^T \mathcal{P}_{m'}^{\frac{1}{2}} \Phi_{m'}(t) \approx H_{m'}^T \mathcal{P}_{m'}^{\frac{1}{2}} \Psi_{m'} \hat{B}_{m'}(t). \end{cases} \tag{18}$$

Then, from (13) and (18), we obtain

$$\int_0^t y_1(s)ds \approx \int_0^t G_{m'}^T \mathcal{P}_{m'}^{\frac{1}{2}} \Phi_{m'}(s)ds = G_{m'}^T \mathcal{P}_{m'}^{\frac{1}{2}} \int_0^t \Phi_{m'}(s)ds \tag{19}$$
$$\approx G_{m'}^T \mathcal{P}_{m'}^{\frac{1}{2}} \mathcal{P}_{m'}^1 \Phi_{m'}(t) \approx G_{m'}^T \mathcal{P}_{m'}^{1+\frac{1}{2}} \Psi_{m'} \hat{B}_{m'}(t),$$

and similarly

$$\int_0^t y_2(s)ds \approx H_{m'}^T \mathcal{P}_{m'}^{1+\frac{1}{2}} \Psi_{m'} \hat{B}_{m'}(t). \tag{20}$$

By replacing (17)–(20) into (16), we obtain

$$\begin{cases} G_{m'}^T \Psi_{m'} \hat{B}_{m'}(t) \\ = \Gamma(\frac{3}{2}) [1, 1, \ldots, 1]_{1 \times m'} \hat{B}_{m'}(t) + (G_{m'}^T \mathcal{P}_{m'}^{1+\frac{1}{2}} \Psi_{m'} + H_{m'}^T \mathcal{P}_{m'}^{1+\frac{1}{2}} \Psi_{m'}) \hat{B}_{m'}(t), \\ H_{m'}^T \Psi_{m'} \hat{B}_{m'}(t) \\ = (G_{m'}^T \mathcal{P}_{m'}^{\frac{1}{2}} \Psi_{m'} + H_{m'}^T \mathcal{P}_{m'}^{\frac{1}{2}} \Psi_{m'}) \hat{B}_{m'}(t) - \Gamma(\frac{3}{2}) [1, 1, \ldots, 1]_{1 \times m'} \hat{B}_{m'}(t). \end{cases} \tag{21}$$

Relation (21) can be rewritten as follows:

$$\begin{cases} G_{m'}^T \Psi_{m'} = \Gamma(\frac{3}{2}) [1, 1, \ldots, 1]_{1 \times m'} + G_{m'}^T \mathcal{P}_{m'}^{1+\frac{1}{2}} \Psi_{m'} + H_{m'}^T \mathcal{P}_{m'}^{1+\frac{1}{2}} \Psi_{m'}, \\ H_{m'}^T \Psi_{m'} = G_{m'}^T \mathcal{P}_{m'}^{\frac{1}{2}} \Psi_{m'} + H_{m'}^T \mathcal{P}_{m'}^{\frac{1}{2}} \Psi_{m'} - \Gamma(\frac{3}{2}) [1, 1, \ldots, 1]_{1 \times m'}. \end{cases} \tag{22}$$

By solving the nonlinear system (22), we can obtain the matrices of coefficients G and H.

In Figure 1, the exact and approximate solutions using the proposed method ($k = 6, M = 2$) are plotted and the numerical values are given in Table 1.
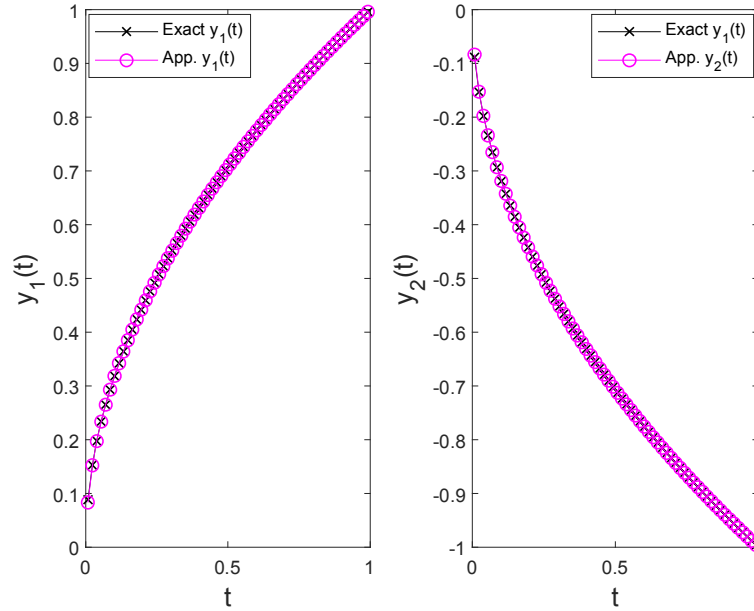

Figure 1: Exact and approximate solution of $y_1(t)$ and $y_2(t)$ in Example 1.

Table 1: Exact and approximate solution and absolute error (AE) for $y_1(t)$ and $y_2(t)$ in Example 1.

t	Ex. $y_1(t)$	Ap. $y_1(t)$	AE $y_1(t)$	Ex. $y_2(t)$	Ap. $y_2(t)$	AE $y_2(t)$
2.3438e-02	1.5309e-01	1.5237e-01	7.2418e-04	-1.5309e-01	-1.5237e-01	7.2418e-04
1.0156e-01	3.1869e-01	3.1861e-01	7.8660e-05	-3.1869e-01	-3.1861e-01	7.8660e-05
1.7969e-01	4.2390e-01	4.2386e-01	3.3400e-05	-4.2390e-01	-4.2386e-01	3.3400e-05
2.5781e-01	5.0775e-01	5.0773e-01	1.9431e-05	-5.0775e-01	-5.0773e-01	1.9431e-05
3.3594e-01	5.7960e-01	5.7959e-01	1.3062e-05	-5.7960e-01	-5.7959e-01	1.3062e-05
4.1406e-01	6.4348e-01	6.4347e-01	9.5455e-06	-6.4348e-01	-6.4347e-01	9.5455e-06
4.9219e-01	7.0156e-01	7.0155e-01	7.3654e-06	-7.0156e-01	-7.0155e-01	7.3654e-06
5.7031e-01	7.5519e-01	7.5518e-01	5.9049e-06	-7.5519e-01	-7.5518e-01	5.9049e-06
6.4844e-01	8.0526e-01	8.0525e-01	4.8706e-06	-8.0526e-01	-8.0525e-01	4.8706e-06
7.2656e-01	8.5239e-01	8.5238e-01	4.1065e-06	-8.5239e-01	-8.5238e-01	4.1065e-06
8.0469e-01	8.9704e-01	8.9704e-01	3.5232e-06	-8.9704e-01	-8.9704e-01	3.5232e-06
8.8281e-01	9.3958e-01	9.3958e-01	3.0660e-06	-9.3958e-01	-9.3958e-01	3.0660e-06
9.7656e-01	9.8821e-01	9.8821e-01	2.6353e-06	-9.8821e-01	-9.8821e-01	2.6353e-06

Example 2. Consider

$$\begin{cases} D^p y_1(t) = \frac{1}{3} y_1(t) y_2(t) + \frac{1}{2} y_2{}^2(t) + 2 y_2(t) - \int_0^t [y_1(s) + y_2(s)] ds, \\ D^q y_2(t) = \frac{1}{3} y_1(t) y_2(t) - y_1(t) + 1 - \int_0^t [y_1(s) - 2 y_2(s)] ds, \end{cases} \quad (23)$$

where $y_1(0) = 0, y_2(0) = 0$, and $0 < p, q \le 1$.

Exact solutions for the above system when $p = q = 1$ are $y_1(t) = t^2$ and $y_2(t) = t$. The exact solutions of $y_1(t)$ and $y_2(t)$ for $p, q \in (0,1)$ are unknown. Let

$$D^p y_1(t) \approx U_{m'}^T \Phi_{m'}(t), \quad D^q y_2(t) \approx V_{m'}^T \Phi_{m'}(t), \quad (24)$$

where

$$U_{m'}^T = [u_1, u_2, u_3, \dots, u_{m'}], \quad V_{m'}^T = [v_1, v_2, v_3, \dots, v_{m'}].$$

By using the initial conditions and (2), (14), (15), and (24), we have

$$\begin{cases} y_1(t) = I^p D^p y_1(t) + y_1(0) \approx U_{m'}^T \mathcal{P}_{m'}^p \Phi_{m'}(t) \approx U_{m'}^T \mathcal{P}_{m'}^p \Psi_{m'} \hat{B}_{m'}(t), \\ y_2(t) = I^q D^q y_2(t) + y_2(0) \approx V_{m'}^T \mathcal{P}_{m'}^q \Phi_{m'}(t) \approx V_{m'}^T \mathcal{P}_{m'}^q \Psi_{m'} \hat{B}_{m'}(t). \end{cases} \quad (25)$$

Then, from (10), (11), (13), and (25), we obtain

$$\begin{aligned} y_1(t) y_2(t) &\approx (U_{m'}^T \mathcal{P}_{m'}^p \Psi_{m'} \hat{B}_{m'}(t))(V_{m'}^T \mathcal{P}_{m'}^q \Psi_{m'} \hat{B}_{m'}(t)) \\ &= (U_{m'}^T \mathcal{P}_{m'}^p \Psi_{m'} \otimes V_{m'}^T \mathcal{P}_{m'}^q \Psi_{m'}) \hat{B}_{m'}(t), \end{aligned} \quad (26)$$

$$y_2^2(t) \approx \left(V_{m'}^T \mathcal{P}_{m'}^q \Psi_{m'} \hat{B}_{m'}(t)\right)^2 = (V_{m'}^T \mathcal{P}_{m'}^q \Psi_{m'})^2 \hat{B}_{m'}(t), \quad (27)$$

$$\begin{aligned} \int_0^t y_1(s) ds &\approx \int_0^t U_{m'}^T \mathcal{P}_{m'}^p \Phi_{m'}(s) ds = U_{m'}^T \mathcal{P}_{m'}^p \int_0^t \Phi_{m'}(s) ds \\ &\approx U_{m'}^T \mathcal{P}_{m'}^p \mathcal{P}_{m'}^1 \Phi_{m'}(t) \approx U_{m'}^T \mathcal{P}_{m'}^{1+p} \Psi_{m'} \hat{B}_{m'}(t), \end{aligned} \quad (28)$$

and in the same way

$$\int_0^t y_2(s) ds \approx V_{m'}^T \mathcal{P}_{m'}^{1+q} \Psi_{m'} \hat{B}_{m'}(t). \quad (29)$$

By replacing (24) and (26)–(29) into (23), we obtain

$$\begin{cases} U_{m'}^T \Psi_{m'} \hat{B}_{m'}(t) = & \frac{1}{3}(U_{m'}^T \mathcal{P}_{m'}^p \Psi_{m'} \otimes V_{m'}^T \mathcal{P}_{m'}^q \Psi_{m'}) \hat{B}_{m'}(t) \\ & + \frac{1}{2}(V_{m'}^T \mathcal{P}_{m'}^q \Psi_{m'})^2 \hat{B}_{m'}(t) + 2 V_{m'}^T \mathcal{P}_{m'}^q \Psi_{m'} \hat{B}_{m'}(t) \\ & - U_{m'}^T \mathcal{P}_{m'}^{1+p} \Psi_{m'} \hat{B}_{m'}(t) - V_{m'}^T \mathcal{P}_{m'}^{1+q} \Psi_{m'} \hat{B}_{m'}(t), \\ \\ V_{m'}^T \Psi_{m'} \hat{B}_{m'}(t) = & \frac{1}{3}(U_{m'}^T \mathcal{P}_{m'}^p \Psi_{m'} \otimes V_{m'}^T \mathcal{P}_{m'}^q \Psi_{m'}) \hat{B}_{m'}(t) \\ & - U_{m'}^T \mathcal{P}_{m'}^p \Psi_{m'} \hat{B}_{m'}(t) + [1, 1, \dots, 1]_{1 \times m'} \hat{B}_{m'}(t) \\ & - U_{m'}^T \mathcal{P}_{m'}^{1+p} \Psi_{m'} \hat{B}_{m'}(t) + 2 V_{m'}^T \mathcal{P}_{m'}^{1+q} \Psi_{m'} \hat{B}_{m'}(t). \end{cases} \quad (30)$$

Relation (30) can be rewritten as follows:

$$
\begin{cases}
U_{m'}^T \Psi_{m'} = & \frac{1}{3}(U_{m'}^T \mathcal{P}_{m'}^p \Psi_{m'} \otimes V_{m'}^T \mathcal{P}_{m'}^q \Psi_{m'}) + \frac{1}{2}(V_{m'}^T \mathcal{P}_{m'}^q \Psi_{m'})^2 \\
& + 2V_{m'}^T \mathcal{P}_{m'}^q \Psi_{m'} - U_{m'}^T \mathcal{P}_{m'}^{1+p} \Psi_{m'} \hat{B}_{m'}(t) - V_{m'}^T \mathcal{P}_{m'}^{1+q} \Psi_{m'}, \\
\\
V_{m'}^T \Psi_{m'} = & \frac{1}{3}(U_{m'}^T \mathcal{P}_{m'}^p \Psi_{m'} \otimes V_{m'}^T \mathcal{P}_{m'}^q \Psi_{m'}) - U_{m'}^T \mathcal{P}_{m'}^p \Psi_{m'} \hat{B}_{m'}(t) \\
& + \left[1, 1, \dots, 1\right]_{1 \times m'} - U_{m'}^T \mathcal{P}_{m'}^{1+p} \Psi_{m'} + 2V_{m'}^T \mathcal{P}_{m'}^{1+q} \Psi_{m'}.
\end{cases}
\tag{31}
$$

By solving the nonlinear system (31), we can obtain the matrices of coefficients U and V. In Figure 2, the exact solutions for $p = q = 1$ and approximate solutions for different values of p and q are plotted. In Figure 2, the approximate values are obtained by using the proposed method ($k = 5, M = 3$), and also the numerical values are given in Tables 2 and 3.
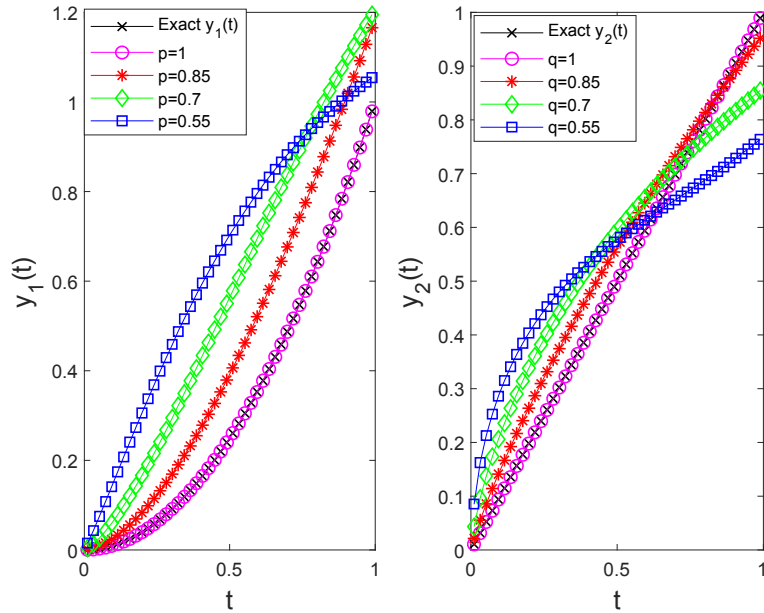

Figure 2: Numerical solution of $y_1(t)$ and $y_2(t)$ for different values p and q in Example 1.

Example 3. Consider

$$
\begin{cases}
D^p y_1(t) = y_1^2(t) + y_2^2(t) - \int_0^t y_1(s)ds, \\
D^q y_2(t) = -\frac{1}{2}y_2^2(t) - y_1(t) + \frac{1}{2} + \int_0^t y_1(s)y_2(s)ds,
\end{cases}
\tag{32}
$$

where $y_1(0) = 0, y_2(0) = 1$ and $0 < p, q \le 1$.

Table 2: Exact and approximate solution and absolute error (AE) for $y_1(t)$ in Example 1.

t	Ex.[p = 1]	Ap.[p = 1]	AE[p = 1]	Ap.[p = 0.85]	Ap.[p = 0.7]	Ap.[p = 0.55]
1.0417e-02	1.0851e-04	2.1680e-04	1.0829e-04	9.0701e-04	3.7273e-03	1.4986e-02
9.3750e-02	8.7891e-03	8.8949e-03	1.0582e-04	2.3452e-02	5.9316e-02	1.4077e-01
1.7708e-01	3.1359e-02	3.1460e-02	1.0172e-04	6.8756e-02	1.4291e-01	2.7310e-01
2.6042e-01	6.7817e-02	6.7913e-02	9.5890e-05	1.3193e-01	2.4150e-01	3.9923e-01
3.4375e-01	1.1816e-01	1.1825e-01	8.8208e-05	2.1044e-01	3.4943e-01	5.1564e-01
4.2708e-01	1.8240e-01	1.8248e-01	7.8552e-05	3.0242e-01	4.6286e-01	6.2076e-01
5.1042e-01	2.6053e-01	2.6059e-01	6.6793e-05	4.0627e-01	5.7884e-01	7.1406e-01
5.9375e-01	3.5254e-01	3.5259e-01	5.2791e-05	5.2059e-01	6.9495e-01	7.9567e-01
6.7708e-01	4.5844e-01	4.5848e-01	3.6398e-05	6.4402e-01	8.0916e-01	8.6627e-01
7.6042e-01	5.7823e-01	5.7825e-01	1.7458e-05	7.7524e-01	9.1976e-01	9.2690e-01
8.4375e-01	7.1191e-01	7.1191e-01	4.1961e-06	9.1295e-01	1.0253e+00	9.7893e-01
9.2708e-01	8.5948e-01	8.5945e-01	2.8742e-05	1.0558e+00	1.1248e+00	1.0240e+00
9.8958e-01	9.7928e-01	9.7923e-01	4.9161e-05	1.1656e+00	1.1950e+00	1.0543e+00

Table 3: Exact and approximate solution and absolute error (AE) for $y_2(t)$ in Example 1.

t	Ex.[q = 1]	Ap.[q = 1]	AE[q = 1]	Ap.[q = 0.85]	Ap.[q = 0.7]	Ap.[q = 0.55]
1.0417e-02	1.0417e-02	1.0416e-02	7.5926e-07	2.1272e-02	4.2951e-02	8.5180e-02
9.3750e-02	9.3750e-02	9.3743e-02	7.0114e-06	1.4078e-01	2.0576e-01	2.8594e-01
1.7708e-01	1.7708e-01	1.7707e-01	1.3592e-05	2.4035e-01	3.1438e-01	3.8446e-01
2.6042e-01	2.6042e-01	2.6040e-01	2.0462e-05	3.3126e-01	4.0256e-01	4.5249e-01
3.4375e-01	3.4375e-01	3.4372e-01	2.7585e-05	4.1619e-01	4.7775e-01	5.0415e-01
4.2708e-01	4.2708e-01	4.2705e-01	3.4929e-05	4.9638e-01	5.4348e-01	5.4588e-01
5.1042e-01	5.1042e-01	5.1037e-01	4.2466e-05	5.7259e-01	6.0188e-01	5.8140e-01
5.9375e-01	5.9375e-01	5.9370e-01	5.0169e-05	6.4530e-01	6.5441e-01	6.1329e-01
6.7708e-01	6.7708e-01	6.7703e-01	5.8012e-05	7.1488e-01	7.0223e-01	6.4344e-01
7.6042e-01	7.6042e-01	7.6035e-01	6.5975e-05	7.8160e-01	7.4628e-01	6.7336e-01
8.4375e-01	8.4375e-01	8.4368e-01	7.4034e-05	8.4566e-01	7.8743e-01	7.0429e-01
9.2708e-01	9.2708e-01	9.2700e-01	8.2170e-05	9.0727e-01	8.2650e-01	7.3726e-01
9.8958e-01	9.8958e-01	9.8950e-01	8.8310e-05	9.5195e-01	8.5492e-01	7.6385e-01

Exact solutions for the above system when $p = q = 1$ are $y_1(t) = \sin(t)$ and $y_2(t) = \cos(t)$. The exact solutions of $y_1(t)$ and $y_2(t)$ for $p, q \in (0, 1)$ are unknown.
Let

$$D^p y_1(t) \approx W_{m'}^T \Phi_{m'}(t), \quad D^q y_2(t) \approx R_{m'}^T \Phi_{m'}(t), \tag{33}$$

where

$$W_{m'}^T = [w_1, w_2, w_3, \ldots, w_{m'}], \quad R_{m'}^T = [r_1, r_2, r_3, \ldots, r_{m'}].$$

By using the initial conditions and (2), (14), (15), and (33), we have

$$\begin{cases} y_1(t) = I^p D^p y_1(t) + y_1(0) \approx W_{m'}^T \mathcal{P}_{m'}^p \Phi_{m'}(t) \approx W_{m'}^T \mathcal{P}_{m'}^p \Psi_{m'} \hat{B}_{m'}(t), \\ y_2(t) = I^q D^q y_2(t) + y_2(0) \approx R_{m'}^T \mathcal{P}_{m'}^q \Phi_{m'}(t) + 1 \approx R_{m'}^T \mathcal{P}_{m'}^q \Psi_{m'} \hat{B}_{m'}(t) + 1, \end{cases} \tag{34}$$

Then, from (10), (11), (13), and (34), we obtain

$$y_1(t)y_2(t) \approx (W_{m'}^T \mathcal{P}_{m'}^p \Psi_{m'} \hat{B}_{m'}(t))(R_{m'}^T \mathcal{P}_{m'}^q \Psi_{m'} \hat{B}_{m'}(t) + 1)$$
$$= (W_{m'}^T \mathcal{P}_{m'}^p \Psi_{m'} \otimes R_{m'}^T \mathcal{P}_{m'}^q \Psi_{m'}) \hat{B}_{m'}(t) + W_{m'}^T \mathcal{P}_{m'}^p \Psi_{m'} \hat{B}_{m'}(t),$$

(35)

$$y_1^2(t) \approx (W_{m'}^T \mathcal{P}_{m'}^p \Psi_{m'})^2 \hat{B}_{m'}(t),$$

$$y_2^2(t) \approx (R_{m'}^T \mathcal{P}_{m'}^q \Psi_{m'})^2 \hat{B}_{m'}(t) + 2R_{m'}^T \mathcal{P}_{m'}^q \Psi_{m'} \hat{B}_{m'}(t) + 1,$$

(36)

$$\int_0^t y_1(s)ds \approx \int_0^t W_{m'}^T \mathcal{P}_{m'}^p \Phi_{m'}(s)ds \approx W_{m'}^T \mathcal{P}_{m'}^{1+p} \Psi_{m'} \hat{B}_{m'}(t), \qquad (37)$$

$$\int_0^t y_1(s)y_2(s)ds \approx \int_0^t (W_{m'}^T \mathcal{P}_{m'}^p \Psi_{m'} \otimes R_{m'}^T \mathcal{P}_{m'}^q \Psi_{m'}) \hat{B}_{m'}(s)ds$$

$$+ \int_0^t W_{m'}^T \mathcal{P}_{m'}^p \Psi_{m'}(s) \hat{B}_{m'}(s)ds$$

$$= (W_{m'}^T \mathcal{P}_{m'}^p \Psi_{m'} \otimes R_{m'}^T \mathcal{P}_{m'}^q \Psi_{m'}) \int_0^t \hat{B}_{m'}(s)ds$$

$$+ W_{m'}^T \mathcal{P}_{m'}^p \Psi_{m'} \int_0^t \hat{B}_{m'}(s)ds \qquad (38)$$

$$\approx (W_{m'}^T \mathcal{P}_{m'}^p \Psi_{m'} \otimes R_{m'}^T \mathcal{P}_{m'}^q \Psi_{m'}) \int_0^t \Psi_{m'}^{-1} \Phi_{m'}(s)ds$$

$$+ W_{m'}^T \mathcal{P}_{m'}^p \Psi_{m'} \int_0^t \Psi_{m'}^{-1} \Phi_{m'}(s)ds$$

$$\approx (W_{m'}^T \mathcal{P}_{m'}^p \Psi_{m'} \otimes R_{m'}^T \mathcal{P}_{m'}^q \Psi_{m'}) \Psi_{m'}^{-1} \mathcal{P}_{m'} \Psi_{m'} \hat{B}_{m'}(t)$$

$$+ W_{m'}^T \mathcal{P}_{m'}^{1+p} \Psi_{m'} \hat{B}_{m'}(t).$$

By replacing (33)–(38) into (32), we obtain

$$\begin{cases} W_{m'}^T \Psi_{m'} = & (W_{m'}^T \mathcal{P}_{m'}^p \Psi_{m'})^2 + (R_{m'}^T \mathcal{P}_{m'}^q \Psi_{m'})^2 \\ & + 2R_{m'}^T \mathcal{P}_{m'}^q \Psi_{m'} - W_{m'}^T \mathcal{P}_{m'}^{1+p} \Psi_{m'} + \left[1, 1, \ldots, 1\right]_{1 \times m'}, \\ \\ R_{m'}^T \Psi_{m'} = & -\frac{1}{2}(R_{m'}^T \mathcal{P}_{m'}^q \Psi_{m'})^2 - R_{m'}^T \mathcal{P}_{m'}^q \Psi_{m'} - W_{m'}^T \mathcal{P}_{m'}^p \Psi_{m'} \\ & - (W_{m'}^T \mathcal{P}_{m'}^p \Psi_{m'} \otimes R_{m'}^T \mathcal{P}_{m'}^q \Psi_{m'} + W_{m'}^T \mathcal{P}_{m'}^p \Psi_{m'}) \Psi_{m'}^{-1} \mathcal{P}_{m'} \Psi_{m'}. \end{cases}$$

(39)

By solving the nonlinear system (39), we can obtain the matrices of coefficients W and R. In Figure 3, the exact solutions for $p = q = 1$ and approximate solutions for different values of p and q are plotted. In Figure 3, the approximate values are obtained by using the proposed method ($k = 4, M = 6$), and also the numerical values are given in Tables 4 and 5.
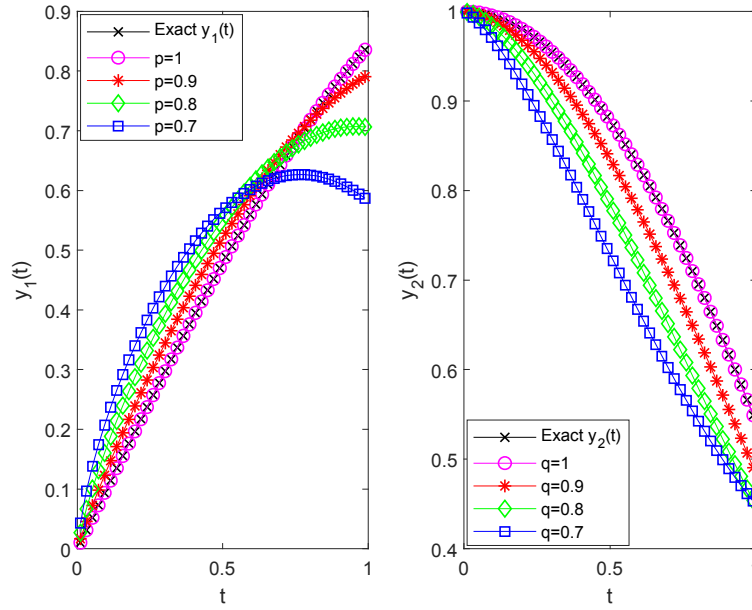
Figure 3: Numerical solution of $y_1(t), y_2(t)$ for different values p and q in Example 2.

Table 4: Exact and approximate solution and absolute error (AE) for $y_1(t)$ in Example 2.

t	Ex.$[p = 1]$	Ap.$[p = 1]$	AE $[p = 1]$	Ap.$[p = 0.9]$	Ap.$[p = 0.8]$	Ap.$[q = 0.7]$
1.0417e-02	1.0416e-02	1.0415e-02	1.6952e-06	1.6784e-02	2.6928e-02	4.2987e-02
9.3750e-02	9.3613e-02	9.3597e-02	1.5248e-05	1.2310e-01	1.6051e-01	2.0698e-01
1.7708e-01	1.7616e-01	1.7613e-01	2.8760e-05	2.1677e-01	2.6388e-01	3.1639e-01
2.6042e-01	2.5748e-01	2.5744e-01	4.2191e-05	3.0362e-01	3.5318e-01	4.0297e-01
3.4375e-01	3.3702e-01	3.3696e-01	5.5500e-05	3.8452e-01	4.3146e-01	4.7285e-01
4.2708e-01	4.1422e-01	4.1415e-01	6.8655e-05	4.5957e-01	4.9979e-01	5.2851e-01
5.1042e-01	4.8854e-01	4.8846e-01	8.1641e-05	5.2857e-01	5.5854e-01	5.7118e-01
5.9375e-01	5.5947e-01	5.5938e-01	9.4461e-05	5.9123e-01	6.0778e-01	6.0154e-01
6.7708e-01	6.2652e-01	6.2642e-01	1.0715e-04	6.4720e-01	6.4744e-01	6.1997e-01
7.6042e-01	6.8922e-01	6.8910e-01	1.1978e-04	6.9609e-01	6.7729e-01	6.2671e-01
8.4375e-01	7.4714e-01	7.4701e-01	1.3249e-04	7.3749e-01	6.9709e-01	6.2197e-01
9.2708e-01	7.9987e-01	7.9973e-01	1.4544e-04	7.7098e-01	7.0653e-01	6.0602e-01
9.8958e-01	8.3580e-01	8.3564e-01	1.5548e-04	7.9065e-01	7.0661e-01	5.8697e-01

Table 5: Exact and approximate solution and absolute error (AE) for $y_2(t)$ in Example 2.

t	Ex.[$q = 1$]	Ap.[$q = 1$]	AE[$q = 1$]	Ap.[$q = 0.85$]	Ap.[$q = 0.7$]	Ap.[$q = 0.55$]
1.0417e-02	9.9995e-01	9.9989e-01	5.4234e-05	9.9972e-01	9.9927e-01	9.9815e-01
9.3750e-02	9.9561e-01	9.9556e-01	5.3356e-05	9.9152e-01	9.8413e-01	9.7089e-01
1.7708e-01	9.8436e-01	9.8431e-01	5.1034e-05	9.7364e-01	9.5657e-01	9.3023e-01
2.6042e-01	9.6628e-01	9.6624e-01	4.7223e-05	9.4758e-01	9.2039e-01	8.8251e-01
3.4375e-01	9.4150e-01	9.4146e-01	4.1891e-05	9.1427e-01	8.7751e-01	8.3059e-01
4.2708e-01	9.1018e-01	9.1014e-01	3.5016e-05	8.7448e-01	8.2939e-01	7.7641e-01
5.1042e-01	8.7254e-01	8.7251e-01	2.6593e-05	8.2892e-01	7.7726e-01	7.2155e-01
5.9375e-01	8.2885e-01	8.2883e-01	1.6622e-05	7.7829e-01	7.2227e-01	6.6736e-01
6.7708e-01	7.7940e-01	7.7940e-01	5.1134e-06	7.2329e-01	6.6547e-01	6.1505e-01
7.6042e-01	7.2455e-01	7.2456e-01	7.9178e-06	6.6465e-01	6.0790e-01	5.6571e-01
8.4375e-01	6.6467e-01	6.6469e-01	2.2457e-05	6.0308e-01	5.5059e-01	5.2032e-01
9.2708e-01	6.0017e-01	6.0021e-01	3.8493e-05	5.3936e-01	4.9452e-01	4.7980e-01
9.8958e-01	5.4904e-01	5.4909e-01	5.1503e-05	4.9063e-01	4.5390e-01	4.5307e-01

5 Conclusion

In this paper, we introduced the Müntz Legendre wavelets to approximate the solution of a system of FIDEs and examined it by some numerical examples. Calculated absolute errors for different values of k and M indicated that by increasing k and M, the absolute errors decrease. The algorithm presented here can be easily used for different types of FIDEs.

References

1. Arikoglu, A. and Ozkol, I. *Solution of fractional integro-differential equations by using fractional differential transform method*, Chaos Solitons Fractals 40 (2009), 521–529.

2. Aslefallah, M. and Rostamy, D. *A numerical scheme for solving space-fractional equation by finite differences theta-method*, Int. J. Adv. Appl. Math. Mech. 1 (4) (2014), 1–9.

3. Aslefallah, M., Rostamy, D., and Hosseinkhani, K. *Solving time-fractional differential diffusion equation by theta-method*, Int. J. Adv. Appl. Math. Mech. 2 (1) (2014), 1–8.

4. Babolian, E., Maleknejad, K., and Mordad, M. *A numerical method for solving Fredholm-Volterra integral equations in two-dimensional spaces using block pulse functions and an operational matrix*, J. Comput. Appl. Math. 235 (14) (2011), 3965–3971.

5. Bahmanpour, M., Tavassoli Kajani, M., and Maleki, M. *Solving Fredholm integral equations of the first kind using Müntz wavelets*, Appl. Numer. Math. 143 (2019), 159–171.

6. Biazar, J., and Ebrahimi, H. *Chebyshev wavelets approach for non-linear systems of Volterra integral equations*, Comput. Math. with Appl. 63 (2012), 608–616.

7. Ebadian, A. and Khajehnasiri, A.A. *Block-pulse functions and their applications to solving systems of higher-order nonlinear Volterra integro-differential equations*, Electron. J. Differ. Equ. 54 (2014), 1–9.

8. Esmaeili, S., Shamsi, M., and Luchko, Y. *Numerical solution of fractional differential equations with a collocation method based on Müntz polynomials*, Comput. Math. Appl. 62(3) (2011), 918–929.

9. Hashim, I. *Adomian decomposition method for solving BVPs for fourth-order integro-differential equations*, J. Comput. Appl. Math. 193 (2006), 658–64.

10. He, J.H. *Approximation analytical solution for seepage flow with fractional derivatives in porous media*, Comput. Methods Appl. Mech. Eng. 167 (1988), 57–68.

11. Hilfer, R. *Applications of fractional calculus in physics*, World Scientific, Singapore, 2000.

12. Huang, L., Li, X.F., and Zhao, Y.L. *Approximate solution of fractional integro-differential equations by Taylor expansion method*, Comput. Math. Appl. 62 (2011), 1127–1134.

13. Keshavarz, E., Ordokhani, Y., and Razzaghi, M. *Bernoulli wavelet operational matrix of fractional order integration and its applications in solving the fractional order differential equations*, Appl. Math. Model. 38 (2014), 6038–6051.

14. Khader, M.M. *Numerical treatment for solving fractional Riccati differential equations*, J. Egypt Math. Soc. 21 (2013), 32–37.

15. Li, Y.L. and Sun, N. *Numerical solution of fractional differential equations using the generalized block pulse operational matrix*, Comput. Math. Appl. 62 (2011), 1046–1054.

16. Ma, X.H. and Huang, C.M. *Spectral collocation method for linear fractional integro-differential equations*, Appl. Math. Model. 38 (2014), 1434–1448.

17. Meerschaert, M.M., Benson, D.A., and Bäumer, B. *Multidimensional advection and fractional dispersion*, Phys. Rev. E 59 (1999), 5026–5028.

18. Mittal, R.C. and Nigam, R. *Solution of fractional calculus and fractional integro-differential equations by Adomian decomposition method*, Int. J. Appl. Math. Mech. 4 (2) (2008), 87–94.

19. Mokhtary, P. and Ghoreishi, F. *The L^2-convergence of the Legendre spectral Tau matrix formulation for nonlinear fractional integro-differential equations*, Numer. Algorithms 58 (2011), 475–496.

20. Mokhtary, P., Ghoreishi, F., and Srivastava, H.M. *The Müntz-Legendre Tau method for fractional differential equations*, Appl. Math. Model. 40 (2016), 671–684.

21. Nadzharyan, T.A., Sorokin, V.V., and Stepanov, G.V. *A fractional calculus approach to modeling rheological behavior of soft magnetic elastomers*, Polymer 92 (2010), 179–188.

22. Nawaz, Y. *Variational iteration method and homotopy perturbation method for fourth-order fractional integro-differential equations*, Comput. Math. Appl. 61 (2011), 2330–2341.

23. Nazari, D.and Shahmorad, S. *Application of the fractional differential transform method to fractional order integro-defferential equations with nonlocal boundary conditions*, J. Comput. Appl. Math. 234 (3) (2010), 883–891.

24. Pinkus, A. *Density in approximation theory*, Surv. Approx. Theory 1 (2005), 1–45.

25. Podlubny, I. *Fractional differential equation*, Academic Press, San Diego, 1999.

26. Rana, S., Bhattacharya, S., and Pal, J. *Paradox of enrichment: A fractional differential approach with memory*, Phys. A Stat. Mech. Appl. 392 (2013), 3610–3621.

27. Sayevand, K., Fardi, M., and Moradi, E. *Convergence analysis of homotopy perturbation method for Volterra integro-differential equations of fractional order*, Alex. Eng. J. 52 (2013), 807–812.

28. Sutulo, S. and Soares, C.G. *On applicability of mathematical models based on fractional calculus to ship dynamics*, in: Proceedings of the Conference on Control Applications in Marine Systems (2010), 15–17.

29. Sweilam, N.H., Khader, M.M., and Al-Bar, R.F. *Numerical studies for a multi-order fractional differential equation*, Phys. Lett. A. 371 (2007) 26–33.

30. Wang, J., Xu, T., Wei, Y., and Xie, J. *Numerical simulation for coupled systems of nonlinear fractional order integro-differential equations via wavelets method*, Appl. Math. Comput. 324 (2018), 36–50.

31. Wang, L.F., Ma, Y.P., and Meng, Z.J. *Haar wavelet method for solving fractional partial differential equations numerically*, Appl. Math. Comput. 227 (2014), 66–76

32. Xie, J., Huang, Q., and Zhao, F. *Numerical solution of nonlinear Volterra–Fredholm–Hammerstein integral equations in two-dimensional spaces based on Block Pulse functions*, J J. Comput. Appl. Math. 317 (2017), 565–572.

33. Xie, J. and Yi, M. *Numerical research of nonlinear system of fractional Volterra-Fredholm integral-differential equations via Block-Pulse functions and error analysis*, J. Comput. Appl. Math. 345 (2019), 159–167.

34. Yang, Y., Chen, Y.P., and Huang, Y.Q. *Convergence analysis of the Jacobi spectral-collocation method for fractional integro-differential equations*, Acta Mathematica Scientia 34B (3) (2014), 673–690.

35. Yi, M.X., Wang, L.F., and Huang, J. *Legendre wavelets method for the numerical solution of fractional integro-differential equations with weakly singular kernel*, Appl. Math. Model. 40 (2016), 3422–3437.

36. Zhang, X.D., Tang, B., and He, Y.N. *Homotopy analysis method for higher-order fractional integro-differential equations*, Comput. Math. Appl. 62 (2011), 3194–3203.

37. Zhu, L. and Fan, Q.B. *Solving fractional nonlinear Fredholm integro-differential equations by the second kind Chebyshev wavelets*, Commun. Nonlinear Sci. Numer. Simul. 17 (2012), 2333–2341.